A compact, robust, and transportable ultra-stable laser with a fractional frequency instability of 1×10^{-15}

Qun-Feng Chen,[1] Alexander Nevsky,[1] Marco Cardace,[1] Stephan Schiller,[1,a)]
Thomas Legero,[2] Sebastian Häfner,[2] Andre Uhde,[2] and Uwe Sterr[2]
[1]*Institut für Experimentalphysik, Heinrich-Heine-Universität Düsseldorf, 40225 Düsseldorf, Germany*
[2]*Physikalisch-Technische Bundesanstalt (PTB), Bundesallee 100, 38116 Braunschweig, Germany*

(Received 5 August 2014; accepted 6 October 2014; published online 12 November 2014)

We present a compact and robust transportable ultra-stable laser system with minimum fractional frequency instability of 1×10^{-15} at integration times between 1 and 10 s. The system was conceived as a prototype of a subsystem of a microwave-optical local oscillator to be used on the satellite mission Space-Time Explorer and QUantum Equivalence Principle Space Test (STE-QUEST) (http://sci.esa.int/ste-quest/). It was therefore designed to be compact, to sustain accelerations occurring during rocket launch, to exhibit low vibration sensitivity, and to reach a low frequency instability. Overall dimensions of the optical system are 40 cm × 20 cm × 30 cm. The acceleration sensitivities of the optical frequency in the three directions were measured to be $1.7 \times 10^{-11}/g$, $8.0 \times 10^{-11}/g$, and $3.9 \times 10^{-10}/g$, and the absolute frequency instability was determined via a three-cornered hat measurement. Two additional cavity-stabilized lasers were used for this purpose, one of which had an instability $\sigma_y < 4 \times 10^{-16}$ at 1 s integration time. The design is also appropriate and useful for terrestrial applications. © *2014 AIP Publishing LLC*. [http://dx.doi.org/10.1063/1.4898334]

I. INTRODUCTION

Space is an ideal place to carry out certain precision experiments, in particular for testing fundamental notions of space and time.[1–6] This results from the possibility of having one or more of the following features for appropriately selected satellite trajectories: long-duration free-fall, a varying distance to Earth or to other planets, a varying speed, or a varying line of sight to the satellite. For example, atomic clocks, including optical clocks, are proposed to be operated in Space for testing the gravitational time dilation or the Shapiro effect. In such missions, ultra-stable lasers are foreseen to be used as the local oscillators to interrogate the atomic transitions.

A laser with ultra-stable frequency is obtained by locking the laser frequency to the resonance of a high-finesse cavity, which makes the fractional frequency instability $\Delta\nu/\nu$ of the laser equal to the cavity's fractional length instability $\Delta L/L$. This latter instability is in practice limited by several factors: the Brownian thermal noise of the cavity, the temperature instability, and the mechanical instability (influenced by environmental seismic and acoustic accelerations) of the setup. Usually, in the laboratory, in order to reduce the influence of the unavoidably present acceleration noise, the cavity is laid on optimized supporting points.[7–9] However, this makes the whole apparatus not easily transportable. For transportable setups, the cavities need to be mechanically locked during transportation or need to be squeezed in a supporting structure.[10] In this case, deformations of the supporting structure also deform the cavity and increase its acceleration sensitivities. In order to reduce this effect, cavities are designed with special, optimized shapes and squeezed at a particular angle.[11,12] Using such squeeze-insensitive designs, cavities can be operated in non-laboratory environments.[13] However, these designs employ approximately cubic cavity shapes which implies that the cavity volume increases by a factor L^3, if the cavity length L is increased, which is necessary, e.g., in order to reduce its thermal noise. Moreover, it is unclear whether the mountings developed so far are robust enough to withstand a rocket launch, a necessary condition for use of the cavity in space. Cavity designs aimed at satisfying this requirement have been developed[14,15] which comprise complex mechanical layouts which rigidly mount the cavity and at the same time decouple it from acceleration induced deformations of the supporting structure.

In the present publication, we report on another candidate design for a space cavity, which uses independent separate rigid mountings for the each of the three translational degrees of freedom, each acting in the corresponding symmetry plane.[16] It is relatively simple in its implementation, and therefore should be of interest also for terrestrial applications in which transportability without large effort is desirable. Moreover, our design is applicable for long and slim cavities, which are thus relatively compact and lightweight. The system we present was developed for use together with a Nd:YAG laser, since commercial space-qualified Nd:YAG lasers with low free-running linewidth and small free-running absolute frequency drift are available (and have flown in space) but is not restricted to it.

Specifically, within the concept of the STE-QUEST (Space-Time Explorer and QUantum Equivalence Principle Space Test) mission,[4] the purpose of the frequency-stabilized Nd:YAG laser is to serve as an optical local oscillator. An erbium-doped fiber laser frequency comb will be used to convert the ultra-stable optical frequency into an ultra-stable microwave signal for interrogation of a cold cesium atomic

a)Electronic mail: Step.Schiller@uni-duesseldorf.de

clock. This microwave is specified with orders of magnitude lower phase noise and short-term frequency instability than the best space-qualified quartz oscillators.

II. DESIGN OF THE REFERENCE CAVITY

The designs of the cavity spacer and support frame are shown in Fig. 1. The dimensions of the approximately cylindrical cavity spacer are 100 mm × 60 mm (length×diameter). The detailed design of the cavity spacer is shown in Fig. 1(a). The spacer is made from standard grade ULE glass. On each end of the spacer a fused silica mirror (ATFilms, Boulder[27]) is optically contacted. The purpose of using fused silica mirrors instead of ULE mirrors is to reduce the thermal noise[17,18] to a calculated instability flicker floor of $\sigma_y = 4 \times 10^{-16}$. The radii of curvature of the mirrors are infinity and 1 m, respectively. The mirrors are 25.4 mm in diameter and 6.35 mm thick and are high-reflectivity-coated for 1064 nm, leading to a measured cavity linewdith of 3.7 kHz and finesse of 400 000. The central 6 mm diameter area of the back side is anti-reflection-coated for the same wavelength. On the back sides of the cavity mirrors, ULE rings (inner/outer diameter 9/25.4 mm, thickness 6 mm) are optically contacted to compensate the thermal expansion caused by the fused silica mirrors.[19]

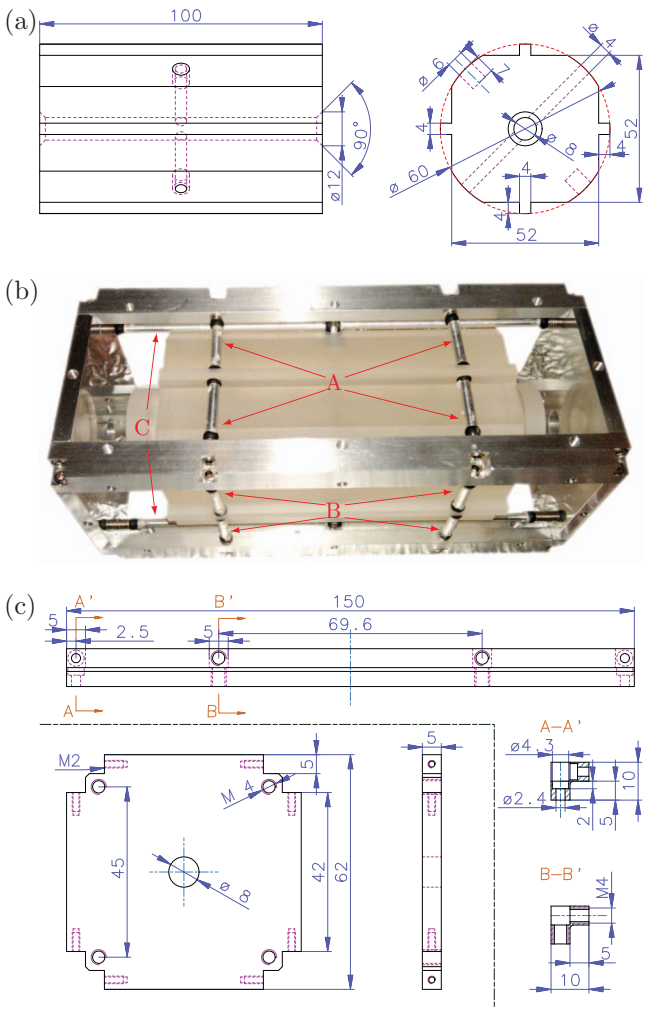

FIG. 1. (a) Technical drawing of the cavity spacer. (b) Photo of the cavity in the supporting frame. (c) Simplified mechanical drawing of the supporting frame. The unit is 1 mm.

The mounting of the cavity is based on the idea to separate the forces acting on the cavity along the optical axis and perpendicular to this direction. The resulting forces are then applied in the corresponding symmetry plane of the cavity. Thus, due to symmetry, to first order in the accelerations a, the resonator length, i.e., the distance between the mirror centers, will not change.[16]

The mounting structure of the cavity is shown in Fig. 1(b). The cavity is supported by squeezing 20 short posts with diameters of 3 mm pairwise on 10 points on the cavity spacer. These 20 posts are divided into 3 groups A, B, and C in Fig. 1(b). The posts in a given group are parallel to each other. Each group restricts the movement of the cavity in the direction parallel to the posts' axes while it allows motion of the cavity in the two directions perpendicular to the posts' axes. For motional constraint in the two directions orthogonal to the cavity axis (groups A and B), 4-post pairs are used for each direction. 2-post pairs are used in order to limit the movement of the cavity along its axis (group C). The distance along the cavity axis between the supporting points in groups B and C are 69.6 mm and they are located symmetrically with respect to the midplane of the cavity which is perpendicular to its axis. The supporting points of group C are on this symmetry plane of the cavity and act on invar pins that are glued into the ULE spacer. The positions of the supporting points were optimized by using finite element simulation.[9,20] M4 set screws on the frame are used to press the posts to the cavity. Viton balls (diameter 4 mm) are inserted between the screws and the posts to reduce the tangential restoring force of the posts. Viton balls cut in half are inserted between the cavity and the posts so as to increase friction and further decouple the cavity from the supporting frame. The mechanical drawing of the supporting frame is shown in Fig. 1(c).

Effects still to consider are deviations from symmetry, e.g., resulting from an offset of the mode axis from the geometrical symmetry axis in combination with acceleration induced bending of the spacer. This bending can be minimized by appropriate positions of the mounting. This was simulated by FEM[21] (Fig. 2) to identify the mounting points with the smallest bending (see Fig. 3). Assuming a 1 mm deviation of the resonator mode from the cavity's geometric symmetry axis, a deviation of the mounting position of 0.5 mm from the optimum position would lead to a sensitivity of $\Delta L/(a\,L) \approx 10^{-11}/g$. Deformation from squeezing the rim at the mounting positions can also couple accelerations to length changes. The FEM simulations indicate a value of $\Delta L/L \approx 10^{-11}$ for a squeezing force of 1 N. To provide reliable holding under a design acceleration of $a_{\max} = 20\,g$, the squeezing force of the mounting needs to be sufficiently large. For a perfectly linear elastic material, the squeezing force needs to balance the maximum reaction force. In our case this would require, for each of the four points in each direction, a squeezing force of 15 N. However, the large-range behavior of viton balls is strongly nonlinear, with the force increasing to the power 3/2 with approach.[22,23] This reduces the required squeezing force by 30% to 10 N. Implementing a higher nonlinearity, e.g., by optimized shape of the viton parts, the

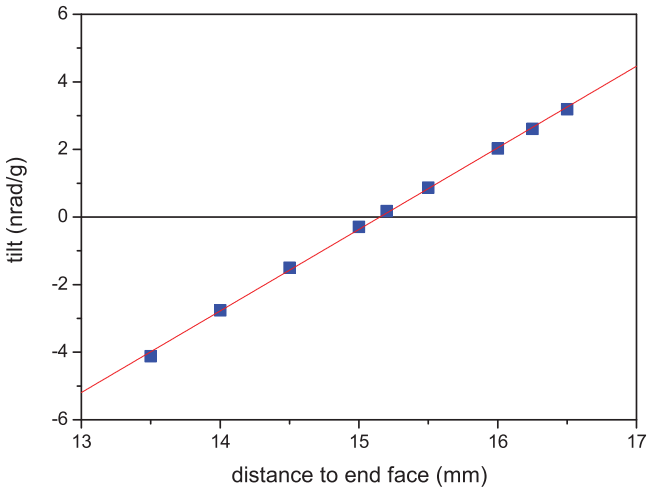

FIG. 2. Tilt of a single end mirror of the cavity as a function of the mounting position under the acceleration $a = 1\ g$ perpendicular to the cavity axis.

squeezing force and related deformation can even be further reduced.

Imperfections on the mount can lead to forces tangential to the mounting plane. On the rim opposite axial forces of 1 N on each pad result in $\Delta x = 6.8 \times 10^{-10}$ m or $\Delta L/L = 13.6 \times 10^{-9}$ and radial forces of 1 N at each pad lead to $\Delta x = 2.19 \times 10^{-10}$ m or $\Delta L/L = 4.38 \times 10^{-9}$ via the Poisson effect. With the cavity mass of 600 g at 1 g acceleration, a total normal force of 6 N needs to be taken up by the supports in group A or B, so these tangential forces need to be less than 10^{-3} of the normal force for a total sensitivity less than $10^{-12}/g$.

III. CAVITY SUBSYSTEM DESCRIPTION

The cavity is operated in a vacuum chamber (VaC) inside two thermal shields. The inner shield is formed by four polished aluminum side covers (4 mm thick, not shown in the figures) that are fixed to the support frame. This assembly is mounted inside the outer thermal shield (TS) by screws

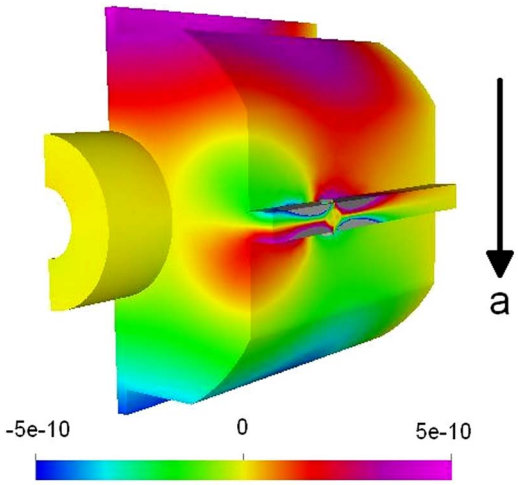

FIG. 3. FEM calculation of deformation in the direction parallel to the optical axis under an acceleration of 1 g. The color code indicates the displacement along the cavity axis (in the unit of meter) and for symmetry reason only one quarter of the cavity was simulated.

and thermally isolating ceramic washers. This outer thermal shield is mounted on 4 thermoelectric cooling elements (TEC1) on the bottom of the vacuum chamber using indium foils to insure good thermal contact between the TEC1 and the thermal shield and the chamber. The TEC1 allows to actively stabilize the temperature of the outer thermal shield to the zero coefficient-of-thermal-expansion (CTE) temperature of the cavity, which was determined to be near 0 °C by measuring the absolute frequency of the cavity by means of a frequency comb when set to different temperatures. Remaining temperature fluctuations of the outer shield are additionally filtered by the inner heat shield, leading to an overall second-order low-pass behavior between the outer shield and the cavity. On long time scales its behavior is described by a time constant of 5.5 h, which was determined by measuring the laser frequency change after a step of the outer shield temperature. To further improve the temperature stability, also the temperature of the vacuum chamber is actively stabilized at 20 °C (with TEC2). All temperature sensors are standard 10 kΩ thermistors and proportional-integral-derivative (PID) control circuits are used to stabilize the temperatures. The in-loop temperature stability at the outer thermal shield is about 1 mK. The vacuum in the chamber is kept to 1×10^{-7} mbar by a miniature 2 l/s ion pump (Gamma Vacuum).

IV. THE OPTICAL SYSTEM

A schematic of the complete system is shown in Fig. 4. A Nd:YAG laser (Innolight, Mephisto S) is frequency-modulated at 3 MHz (G2) via the piezo-actuator (PZT) of the laser. After an optical isolator, the laser beam is coupled to a

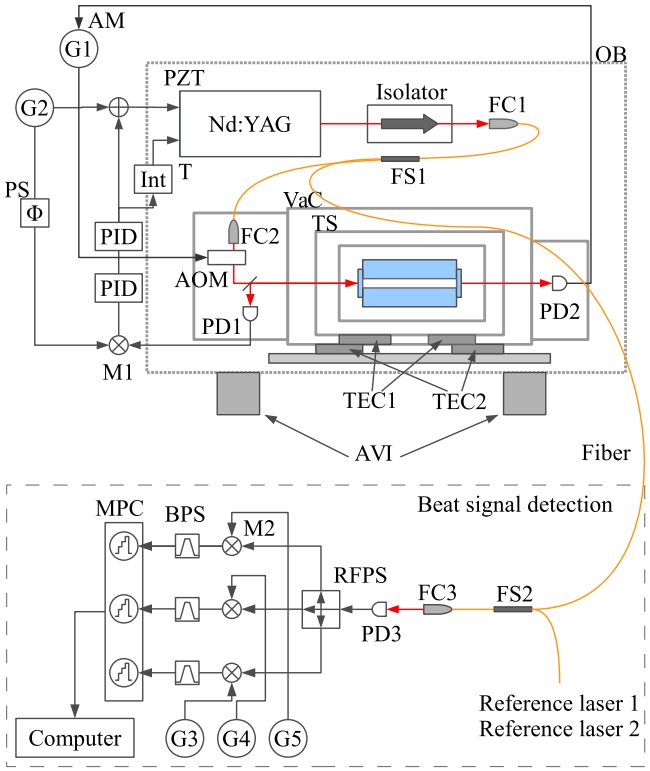

FIG. 4. Schematic of the system. The details of the compact optical setup are shown in Fig. 5 (b). The setup with the abbreviations is described in the main text.

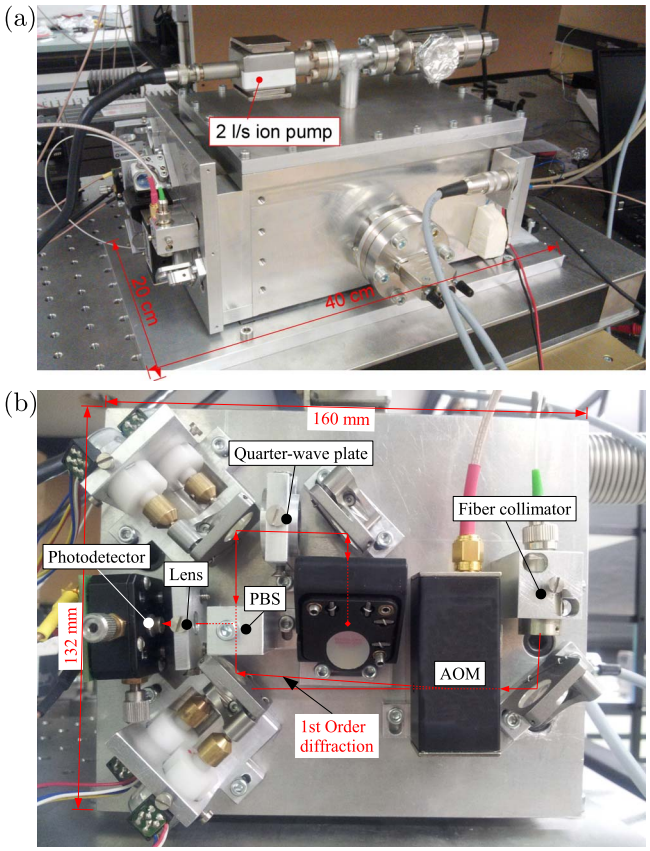

FIG. 5. (a) Overview of the system, with dimensions. (b) The compact optical setup for coupling the laser beam to the cavity and obtaining an error signal.

single-mode fiber by an angled physical contact (APC) fiber collimator (FC, FC1). Using a fiber splitter (FS1) one part of the laser wave is sent to a compact optical breadboard, which is attached to the vacuum chamber, Fig. 5(a), and further coupled into the cavity. The detailed design of the compact breadboard is shown in Fig. 5(b). The laser beam exiting from FC2 is diffracted by the acousto-optic modulator (AOM, Crystal Technology 3200-147). The first-order diffracted wave is coupled into the cavity. The polarizing beam splitter (PBS) and the quarter-wave plate are used to pick up the reflection from the cavity. The lens and the photodetector PD1, mounted on a translation stage are used to detect the reflection from the cavity. The electric signal from the PD1 detector is frequency-mixed (by M1, Mini-Circuits ZAD-8) with the 3 MHz signal, phase-shifted (PS) with respect to the laser modulation signal to generate the error signal. It is filtered by two cascaded PID circuits with P-I corner frequencies of approximately 3 kHz and 10 kHz and P-D corner frequency of approximately 20 kHz and 30 kHz. The output of the locking circuits is combined with the 3 MHz modulation by using a bias-T (Mini-Circuits ZFBT-4R2GW) and fed back to the PZT modulation input of the laser. The output from the second PID is also further integrated (INT) and sent to the temperature control modulation input (T) of the laser for long-term stabilization of the laser.[24] The transmission of the cavity is detected by another detector (PD2) attached to the other side of the vacuum chamber. This signal is used to stabilize the laser power circulating inside the cavity through feedback to the amplitude modulation input (AM) of the AOM driver (G1). The sensitivity of the frequency on the transmitted power is about 500 Hz/μW.

Four stepping motors (Nanotec SPG1518M0504-102) are attached to two of the mirror mounts (New Focus 9876), which may be used to optimize the beam coupling to the cavity when necessary and when there is no manual access to the optical setup, e.g., when during operation in space or at a location on Earth distant from the laboratory. The motors can therefore be omitted when the system is operated in a laboratory with manual access. During initial alignment of the small breadboard, a low-cost CCD camera is set up in transmission through the cavity, in order to identify the cavity modes.

The laser and the optical system are attached to a standard commercial optical breadboard (OB), and placed on an active-vibration-isolation system (AVI, Table-Stable AVI-400). This arrangement is used for testing and characterizing the system, and for operation on Earth. In space, the latter two components would be absent.

The overview of the system is shown in Fig. 5(a). The outer dimensions of the system, without the laser, optical breadboard, and vibration isolation, are about 400 $\times$ 200 $\times$ 300 mm^3 (length$\times$width$\times$height). The mass is approximately 10 kg.

V. CHARACTERIZATION METHOD

The frequency stability of the compact laser system is characterized by beating with two independent ultrastable Nd:YAG lasers whose frequencies are locked to two reference cavities with lengths of 30 cm. The frequency instability of each individual laser is then obtained by the three-cornered-hat method.[25] The laser beam exiting FS1 (Fig. 4) is combined in the fiber splitter FS2 with the two beams from the two reference lasers. The combined beam exiting from FC3 is guided to a fast photo-detector PD3 (EOT ET-3000A), for detecting the three beat signals between the three laser waves. The beat signals (around 70, 480, and 550 MHz) were split into three ways by RFPS (RF power splitter, Mini-Circuits ZF3RSC-542-S+) and down-mixed by three independent synthesizers G3, G4, and G5 (HP 8656B, phase-locked to the same 10 MHz reference) to approximately 10 MHz using mixers M2. Each signal was bandpass-filtered at 10 MHz by BPS (bandpass filter, Mini-Circuits BBP-10.7+) and sent to a four-channel dead-time-free phase comparator MPC (K+K Messtechnik GmbH, FXE). The frequencies are recorded by a computer and analyzed to obtain the Allan deviations.

VI. CHARACTERIZATION RESULTS

We operate the cavity with 200 μW entering the vacuum chamber. The coupling efficiency of the laser wave to the cavity is approximately 40%. The bandwidth of the lock system is about 70 kHz. The system works very reliably and essentially never fell out of lock during several months of operation. The frequency instabilities of the compact laser and the two reference lasers, obtained simultaneously via the three-cornered-hat method are shown in Fig. 6. The lowest

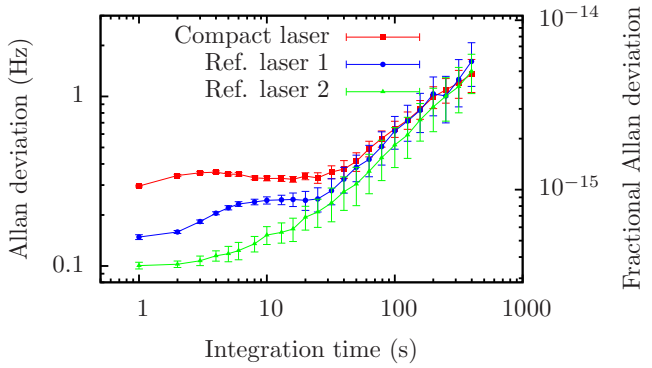

FIG. 6. Allan deviation of the frequency instability of each laser derived with the three-cornered-hat method, when they are frequency-stabilized to independent ULE cavities. The plotted values are the average values of the Allan deviations computed from 10 data intervals of 2000 s duration each, and in which the linear drift was removed in each data interval.

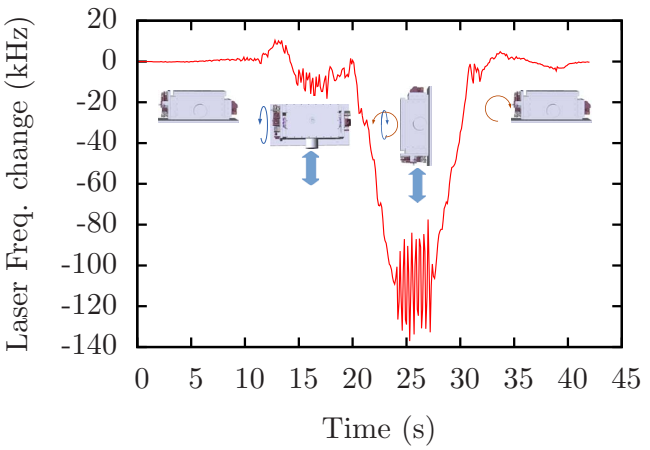

FIG. 8. Laser frequency change while the system is manually reoriented and shaken. The cavity housing images show the orientation and acceleration directions in the different phases of the test. The thin arrows show the rotation direction of the chamber.

instability of the compact laser is 1×10^{-15} for integration times of 1–10 s. It remains below 3×10^{-15} for integration times up to 100 s. This performance satisfies the specification of the STE-QUEST mission[26] which calls for this level for integration times up to 100 s. Note that the most stable of the three laser systems used in the test has an instability of less than 4×10^{-16} at 1 s integration time (green line in Fig. 6).

The acceleration sensitivity coefficients of the cavity are determined by recording acceleration level and beat frequency with respect to one reference laser, while shaking the system (optical system plus optical breadboard placed on AVI, which is supported by springs) sequentially in the three directions. The acceleration level is measured by an acceleration sensor (Wilcoxon research, model 731A) attached to the optical breadboard. The beat frequency is converted to a voltage by a frequency-to-voltage converter (home-built, based on a frequency-to-voltage converter chip, Texas Instruments VFC32KP). The output from the acceleration sensor and the frequency signal are simultaneously recorded by a digital-analog data acquisition card.

An acceleration along the vertical direction was excited by a voice coil actuator (home-built) attached to the optical table and to the optical breadboard and driven at a frequency close to the resonance of the overall system. The acceleration along the two horizontal directions were excited by manually hitting the optical breadboard on the side. From the test, shown in Fig. 7, we obtained acceleration sensitivities along the vertical, the horizontal across-cavity, and the axial directions of $1.7 \times 10^{-11}/g$, $8.0 \times 10^{-11}/g$, and $3.9 \times 10^{-10}/g$, respectively.

For testing the robustness of the system, the system was carried, rotated, and shaken by two persons holding it in their hands. The laser frequency remains stably locked to the cavity. The laser frequency change during this procedure is shown in Fig. 8. The frequency change is about 20 kHz when the cavity is rotated along the cavity axis by 90° (starting at 12 s in the figure), and it is about 100 kHz when the cavity is oriented from the horizontal into the vertical direction (rotation occurs around the horizontal cross-axis, at 40 s). These frequency shifts are consistent with the sensitivities observed in Fig. 7. This test demonstrates that the cavity can be operated vertically or horizontally, and that the mounting concept is quite robust.

Because the cavity and the setup may experience a typical temperature variation from −20 °C to +50 °C during storage and transportation to space, a test of the robustness of the optical setup with respect to temperature variation was also done. The optical setup (without laser and with temperature stabilization switched off) was put in a refrigerator, cooled down to −30 °C, then warmed up to 50 °C with the TEC attached to the vacuum chamber, and finally back to room

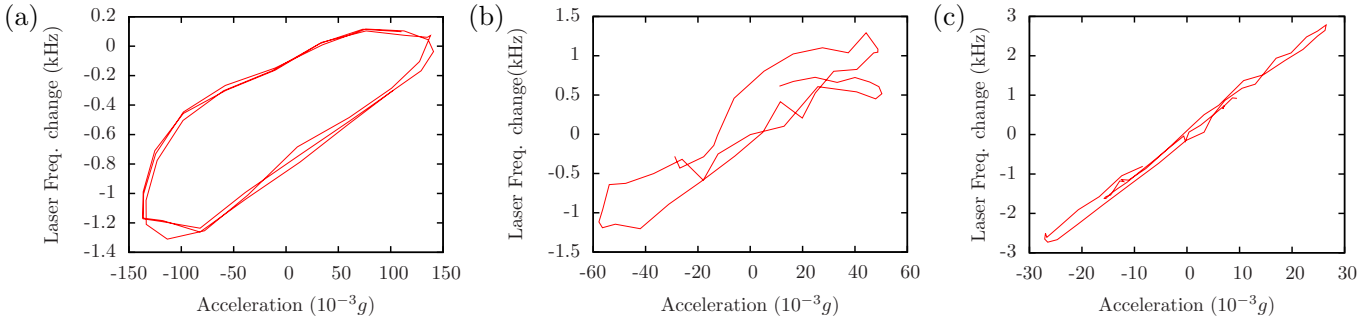

FIG. 7. Relation between the system acceleration and the resulting laser frequency change. The data were taken with sample rates of 200 Hz. The duration of the vibration data plotted were about 0.25 s. (a) The system is shaken in vertical direction, (b) the system is shaken in horizontal direction, and perpendicular to the cavity axis, (c) the system is shaken along the cavity axis.

temperature. The coupling efficiency of the laser beam into the cavity changed from 40% to 15% during this temperature cycle. This means that the alignment was not "lost"; it was brought back to 40% by adjusting just one mirror mount. This was done manually, but, as described above, can in the future also be done by remote control or an automatic routine, using the motorized mirror mounts in the small optical breadboard.

VII. CONCLUSION

In summary, we reported a compact reference cavity based on a robust mounting structure which represents a baseline design for a space unit. In addition, since it does not at present include any particularly sophisticated or expensive elements, the design is also suitable for laboratory use, and for non-laboratory, terrestrial environments. Applications are, e.g., for a transportable optical clock or for a transportable, optically stabilized frequency comb. As an example of a useful application, in our laboratory we routinely use this system as an ultra-stable optical local oscillator to which a fiber frequency comb is locked that measures several other ultra-stable optical frequencies.

ACKNOWLEDGMENTS

This work was funded by the Bundesministerium für Wirtschaft und Technologie (Germany) under Project No. 50OY1201 and the European Metrology Research Programme (EMRP) under IND14. The EMRP is jointly funded by the EMRP participating countries within EURAMET and the European Union (EU). Additional support was provided by the German Science Foundation under Grant Schi 431/20-1.

[1]N. Ashby, P. L. Bender, J. L. Hall, J. Ye, S. A. Diddams, S. R. Jefferts, N. Newbury, C. Oates, R. Dolesi, S. Vitale, and W. J. Weber, in *Relativity in Fundamental Astronomy: Dynamics, Reference Frames, and Data Analysis*, Proc. Int. Astron. Union **5**, 414 (2009).
[2]S. Schiller, G. M. Tino, P. Gill, C. Salomon, U. Sterr, E. Peik, A. Nevsky, A. Görlitz, D. Svehla, G. Ferrari *et al.*, Exp. Astron. **23**, 573 (2009).
[3]P. Wolf, Ch. J. Bordé, A. Clairon, L. Duchayne, A. Landragin, P. Lemonde, G. Santarelli, W. Ertmer, E. Rasel, F. S. Cataliotti *et al.*, Exp. Astron. **23**, 651 (2009).
[4]The Space-Time Explorer and QUantum Equivalence principle Space Test (STE-QUEST), cosmic Vision 2015-2025, the future of ESA's Science Programme, see http://sci.esa.int/ste-quest/.
[5]S. Schiller, A. Görlitz, A. Nevsky, S. Alighanbari, S. Vasilyev, C. Abou-Jaoudeh, G. Mura, T. Franzen, U. Sterr, S. Falke *et al.*, *Proceedings of the 2012 European Frequency and Time Forum (EFTF)*, 24–26 April 2012, Gothenburg, Sweden (IEEE, 2012), pp. 412–418.
[6]B. Altschul, Q. G. Bailey, L. Blanchet, K. Bongs, P. Bouyer, L. Cacciapuoti, S. Capozziello, N. Gaaloul, D. Giulini, J. Hartwig *et al.*, "Quantum tests of the Einstein equivalence principle with the STE-QUEST space mission," e-print arXiv:1404.4307 [Adv. Space Res. (in press)].
[7]T. Nazarova, F. Riehle, and U. Sterr, Appl. Phys. B **83**, 531 (2006).
[8]S. A. Webster, M. Oxborrow, and P. Gill, Phys. Rev. A **75**, 011801 (2007).
[9]J. Millo, D. V. Magalhães, C. Mandache, Y. Le Coq, E. M. L. English, P. G. Westergaard, J. Lodewyck, S. Bize, P. Lemonde, and G. Santarelli, Phys. Rev. A **79**, 053829 (2009).
[10]S. Vogt, C. Lisdat, T. Legero, U. Sterr, I. Ernsting, A. Nevsky, and S. Schiller, Appl. Phys. B **104**, 741 (2011).
[11]S. Webster and P. Gill, Opt. Lett. **36**, 3572–3574 (2011).
[12]D. R. Leibrandt, M. J. Thorpe, M. Notcutt, R. E. Drullinger, T. Rosenband, and J. C. Bergquist, Opt. Express **19**, 3471–3482 (2011).
[13]D. R. Leibrandt, M. J. Thorpe, J. C. Bergquist, and T. Rosenband, Opt. Express **19**, 10278 (2011).
[14]W. M. Folkner, G. deVine, W. M. Klipstein, K. McKenzie, D. Shaddock, R. Spero, R. Thompson, D. Wuchenich, N. Yu, M. Stephens *et al.*, "Laser frequency stabilization for GRACE-II," *Earth Science Technology Forum, Arlington, Virginia*, June 22, 2010 (Jet Propulsion Laboratory, National Aeronautics and Space Administration, 2010), see http://hdl.handle.net/2014/41635.
[15]B. Argence, E. Prevost, T. Lévèque, R. Le Goff, S. Bize, P. Lemonde, and G. Santarelli, Opt. Express **20**, 25409 (2012).
[16]U. Sterr, *Frequenzstabilisierungsvorrichtung*, German patent DE102011015489 B3 (16 August 2012).
[17]K. Numata, A. Kemery, and J. Camp, Phys. Rev. Lett. **93**, 250602 (2004).
[18]T. Kessler, T. Legero, and U. Sterr, J. Opt. Soc. Am. B **29**, 178 (2012).
[19]T. Legero, T. Kessler, and U. Sterr, J. Opt. Soc. Am. B **27**, 914–919 (2010).
[20]L. Chen, J. L. Hall, J. Ye, T. Yang, E. Zang, and T. Li, Phys. Rev. A **74**, 053801 (2006).
[21]*Elmer: Finite Element Software for Multiphysical Problems*, see http://www.csc.fi/elmer/index.phtml.
[22]Y. Tatara, ASM J. Eng. Mater. Technol. **113**, 285 (1991).
[23]Y. Tatara, S. Shima, and J. C. Lucero, ASM J. Eng. Mater. Technol. **113**, 292 (1991).
[24]Q. F. Chen, A. Nevsky, and S. Schiller, Appl. Phys. B **107**, 679 (2012).
[25]J. E. Gray and D. Allan, in *Proceedings of the 28th Annual Symposium on Frequency Control*, 29–31 May 1974, Atlantic City, New Jersey (Electronic Industries Association, Washington, DC, 1974), pp. 243–246, see http://tf.nist.gov/general/pdf/57.pdf.
[26]*STE-QUEST Assessment Study Report (Yellow Book)*, Ref. No. ESA/SRE(2013)6, see http://sci.esa.int/ste-quest/53445-ste-quest-yellow-book/.
[27]This and other information on manufacturers is provided for technical communication purposes only and does not constitute an endorsement by the University of Düsseldorf or PTB.